Methods for measuring work surface illuminance in adaptive solid state lighting networks

Byungkun Lee, Matthew Aldrich, and Joseph A. Paradiso

MIT Media Lab, Responsive Environments Group, Cambridge, MA 02139, USA

ABSTRACT

The inherent control flexibility implied by solid-state lighting – united with the rich details offered by sensor networks – prompts us to rethink lighting control. In this research, we propose several techniques for measuring work surface illuminance and ambient light using a sensor network. The primary goal of this research is to measure work surface illuminance without distraction to the user. We discuss these techniques, including the lessons learned from our prior research. We present a new method for measuring the illuminance contribution of an arbitrary luminaire at the work surface by decomposing the modulated light into its fundamental and harmonic components.

Keywords: Solid state lighting, Fourier analysis, pulse width modulation, sensor networks, adaptive lighting, user control

1. INTRODUCTION

The growing adoption of solid-state lighting enables new forms of interaction with lighting, personalized controls, energy conservation, and new modalities to control and augment the built environment. In this research, we present our latest techniques for measuring, adapting, and controlling solid-state lighting.

In these adaptive systems, a common requirement is measuring the relative contributions of the lighting network at the region of interest. To accomplish this goal, a simple technique is to turn the lights on and off and measure the changes. However, this is distracting. One alternative is to calculate the illuminance indirectly by measuring the attenuation in a non-visible spectrum and transforming the irradiance into illuminance using a predetermined linear model. Other possibilities include a geometric approach, which requires prior knowledge of the position of the luminaires and the size and layout of the operating environment. Yet, we believe it is still possible to use only visible light to accomplish the measurement requirement.

In this paper, we present a technique that utilizes pulse-width modulated LEDs and Fourier analysis to measure the specific attenuation of the fundamental frequency. By ensuring that the fundamental frequency is never aliased with respect to the other light fixtures, we can measure a fixture's contribution without the need to turn any luminaire off completely.

2. RELATED WORK

Increasing research and commercial deployments of sensor networks have motivated the use of networks that monitor lighting conditions and the development of closed-loop lighting control. In these systems, illuminance-sensors are placed (generally in a fixed position) in the area of interest in order to detect the luminance surface and feedback the lighting information.

Park et al. developed a lighting system to create high quality stage lighting to satisfy user profiles and recommends physical sensor placement for better estimation of the light fields.[1] Wen et al. researched fuzzy decision making and Bayesian inference in lighting control networks.[2] Miki et al. studied the tradeoffs between energy consumption and lighting preferences for multiple users using a linear program to calculate the optimal

Further author information: (Send correspondence to M.A.)
B.L.: E-Mail: byungkun@mit.edu
M.A.: E-mail: maldrich@media.mit.edu
J.P.: E-mail: joep@media.mit.edu

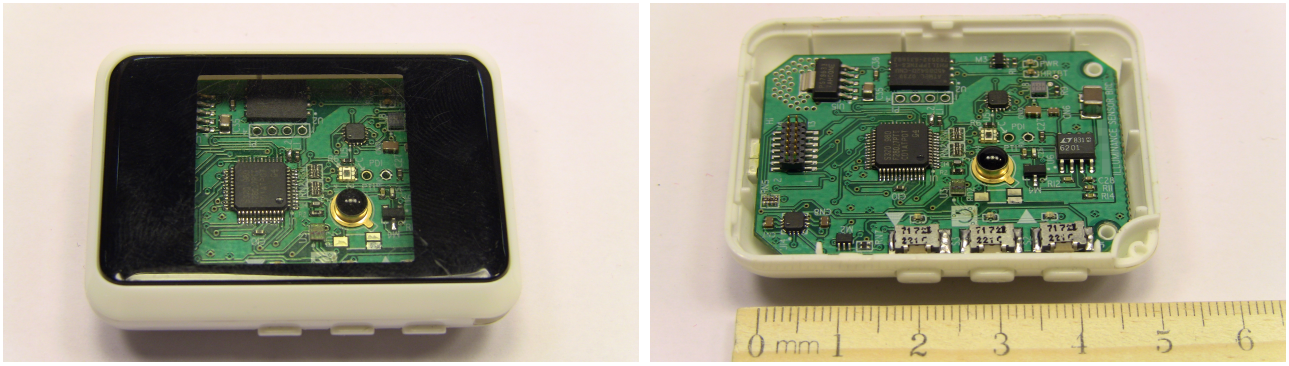

(a) (b)

Figure 1: The second generation sensor with (1a) and without (1b) the lid. The sensor board consists of a 32-bit microcontroller, both digital and analog visible light sensors, an IR-phototransistor, a three-axis accelerometer, external flash memory, and three buttons for controlling intensity and performing a measurement.

intensity settings in a lighting network.[3] Similarly, Pan et. al used a linear program and considered the power consumption as the objective and the user-preference as constraints.[4] Both algorithms require the knowledge of the positions of the occupants, which can be detected using RFID tags or other similar user localization systems.

Recently, increased efficacy and performance of solid-state lighting has reinvigorated interest in intelligent dimming, color control, and networked lighting.[5] Caicedo et al. consider the problem of energy-efficient illumination control based on localized occupancy models. In this work, an occupant's trajectory is modeled as a Markov chain and tracked using ultrasound while a linear program controls the dimming level.[6] Aldrich et al. apply linear and nonlinear optimization to controlling the color and intensity of a LED-based lighting network with the goal of minimizing energy consumption.[7] Wen and Agogino also designed a versatile plug-and-play wireless-networked sensing and actuation system and included a control method incorporating multiple management strategies to provide occupant-specific lighting.[8] Bhardwaj et al. use a predetermined illuminance setting and context (i.e., reading by a lamp) which can compensate for changing ambient light levels or the presence of additional LEDs.[9]

3. MAXIMUM ENERGY EFFICIENCY

Among the applications of a user-friendly lighting system, our project focuses on achieving maximum energy efficiency while providing the desired illuminance to the user. The project solves this problem by finding the optimal power distribution among the light fixtures in the environment. This power distribution can be obtained from an optimizing linear program roughly in the following form:

$$\min_{x_i} \sum_i P_i x_i \quad \text{such that} \quad \begin{cases} \sum_i E_i x_i = E_{desired} \\ 0.05 < x_i < 0.95 \end{cases}$$

This linear program takes the maximum illuminance projected, E_i, and the maximum power consumed, P_i, by each individual light fixture as its coefficients. In order to measure the brightness levels E_i, we developed a photoelectronic receiver (Fig. 1). The receiver affords a high sampling rate, enabling us to record the total illuminance at the receiver and apply some signal processing techniques with respect to time. Since E_i depend on the user's location, they need to be updated every time the user changes position. Once the coefficients are accurately updated, the linear program finds the appropriate values for x_i, the operating ratio of the light fixtures.

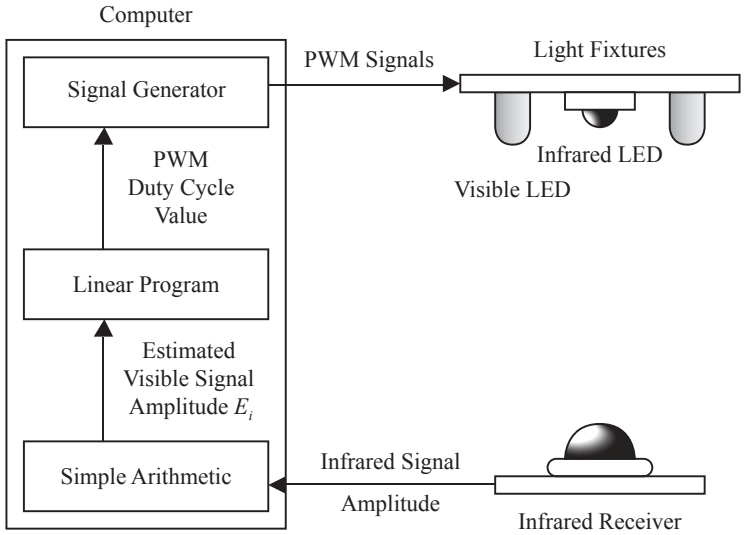

Figure 2: Application of infrared photoelectronic devices.

4. PREVIOUS IMPLEMENTATIONS

Our project from summer 2010 focuses on establishing a method of measuring the coefficients $E_1, E_2, \cdots, E_n$ in real-time while the system is operating. These coefficients need to be updated frequently because the reference point is changed if the user decides to move to another location. Originally, we used an illuminance measurement testbed to find $E_1, E_2, \cdots, E_n$ directly from the maximum illuminance level caused by each individual light fixture at the reference point. This method, however, forces the system to undergo a short calibration period when the contribution level of each individual light is measured by turning on only one light at one time and the others off; even though the period is short, the blinks are certainly noticeable and such blinks recurring every minute may be bothersome for most people. This problem motivated us to develop a new method for calibrating the system without blinking the lights.

We have thus introduced near-infrared LEDs and a detector as a means of solving this problem with a mathematically simplified approach. Since the human eye does not perceive infrared light, we can have the IR components perform the exact same calibration process and leave the visible light on (Fig. 2). The coefficients $E_1, E_2, \cdots, E_n$ are indirectly estimated by simple transfer functions. Over the summer, we laid out a IR receiver daughterboard for the testbed and attached an IR LED to each light fixture. We then performed an experiment to prove the linearity of the receiver circuit, and confirmed the response was indeed linear. In the fall term, we developed a MATLAB code to run a linear program which takes $E_1, E_2, \cdots, E_n$ and yields the optimal PWM duty cycle values. Then, to test them,we connected two LED light fixtures with the IR devices. At the end of the testing process, we confirmed that the IR devices are one possible solution to the blinking problem.

One challenge of using a hybrid visible-NIR system is the potential difficulty involved in matching the IR illumination profile to that of the LED profile. For example, the irradiance and illuminance of the two systems may not intersect the work surface in a similar manner, thus reducing the absolute accuracy of the technique. Although the system is dependent on the physical configuration of the LEDs, proper measurement and profile characterization of the light fixture can account for these differences.

5. FOURIER DOMAIN TECHNIQUES

The goal of our project in spring 2011 is to maintain an unnoticeable calibration processes without the addition of infrared photoelectronic devices. In this approach, we focus on modulated visible light and frequency domain analysis. The assumptions are that: a) the measured fundamental frequency is sufficient in order to estimate the fixture's lighting contribution, and b) the fixture to be measured is set to a unique fundamental frequency relative to the lighting network to prevent aliasing. This distinct frequency will be revealed in the discrete-time Fourier

transform of the signal measured by the receiver since the illuminance level at the receiver is the arithmetic sum of the partial illuminance projected by each individual light fixture.

Our system introduces a PWM signal at half the frequency of normal operation for coefficient measurement. For instance, during the calibration stage, a potential drive signal operates the luminaires at 240 Hz while the light fixture of interest is driven at a hypothetical frequency of 120 Hz. Once the computer evaluates the linear program coefficient E_i, the light fixture is brought back to 240 Hz; then, the next light fixture is moved down to 120 Hz to repeat the same measurement process. Notably, this does not create a discernible difference in luminance since the accumulated average of the intensity over a long duration allows the 240 Hz and the 120 Hz signals to be perceived with the same brightness.

This idea is illustrated in Figure 3. In this example, we consider two hypothetical light fixtures. The fixture we are interested in measuring $x_1(t)$ is set to a 50% duty cycle signal operating at 120 Hz. The other light fixture $x_2(t)$ is also set to a 50% duty cycle but operates at 240 Hz. The PWM waveforms controlling the intensity of the LEDs are given in Figure 3a and Figure 3b. Any optical receiver will not observe these two sources independently. Instead, it will measure the superposition of these two signals. Thus, the receiver measures the quantity $x[n] = x_1[n] + x_2[n]$. The ideal sampled illuminance (no attentuation due to distance) is given in Figure 3c.

By making use of the Fourier transform, this measured signal $x[n]$ can be transformed into $X[k]$, thus revealing the magnitude of the individual fundamental frequencies and harmonic content (Fig. 3d). We now turn our attention to deriving the exact form of $X[k]$ so that we can measure the specific contribution of a light source. In the following discussion, our hypothetical sampling frequency is $f_s = 24$ kHz and the number of samples N measured by the hypothetical receiver is $N = 1000$. In the actual implementation, these values are different given the constraints of the microprocessor.

Take a close look at the graph of $|X[k]|$. By the linearity of discrete Fourier transform, $X[k]$ can be written as the sum $X_1[k] + X_2[k]$, where $X_1[k]$ and $X_2[k]$ are frequency domain representation of $x_1[n]$ and $x_2[n]$, respectively. Since $x_1[n]$ is driven at half of $x_2[n]$'s frequency, $X_1[k]$ has nonzero values at the multiples of 120Hz while $X_2[k]$ has nonzero values only at the multiples of 240Hz. Therefore, the harmonics seen at 120 Hz, 360 Hz, 600 Hz,$\cdots$ are solely determined by $X_1[k]$. The fundamental component at 120Hz, in particular, corresponds to $|X_1[5]|$ since 120 Hz $= 5 \times (f_s = 24 \text{ kHz})/(N = 1000)$.

On the other hand, the first Fourier series coefficient of the original continuous-time signal $x_1(t)$ can be approximated as below:

$$\begin{aligned}
a_1 &= \frac{1}{T}\int_{t_0}^{t_0+T} x(t)\ e^{-j\frac{2\pi}{T}t}\ dt \\
&\approx \frac{1}{T}\sum_{n=n_0}^{n_0+f_sT-1} x[n]\ e^{-j\frac{2\pi}{T}t}\ \Delta t \\
&= \frac{1}{T}\sum_{n=n_0}^{n_0+f_sT-1} x[n]\ e^{-j\frac{2\pi}{T}\frac{n}{f_s}}\ \frac{1}{f_s} \\
&= \frac{1}{f_sT}\sum_{n=n_0}^{n_0+f_sT-1} x[n]\ e^{-j\frac{2\pi}{f_sT}n} \\
&= \frac{1}{N}\sum_{n=n_0}^{n_0+N-1} x[n]\ e^{-j\frac{N}{f_sT}\frac{2\pi}{N}n} \quad \text{if } N \text{ is an integer multiple of } f_sT
\end{aligned} \tag{1}$$

Therefore, we get the relation

$$|a_1| = \left|\left[\frac{N}{f_sT} = 5\right]\right|/(N = 1000) \tag{2}$$

from the above equation. Consequently, we can estimate $|a_1|$ easily by plotting the graph of $|X[k]|$, finding the nearest peak from the center, and then dividing it by the total number N of samples. Notice that the length

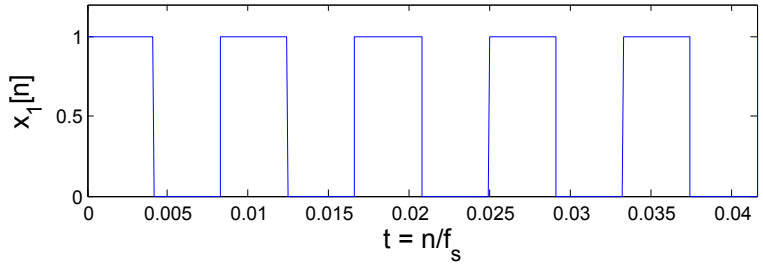

(a)

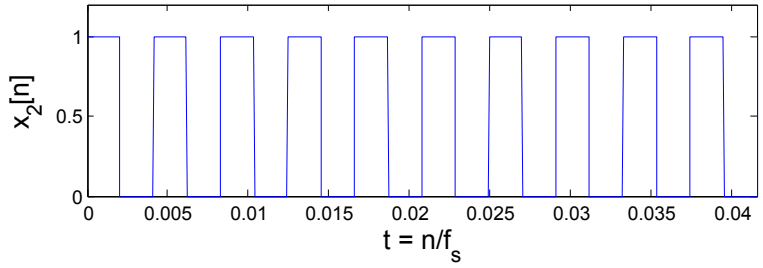

(b)

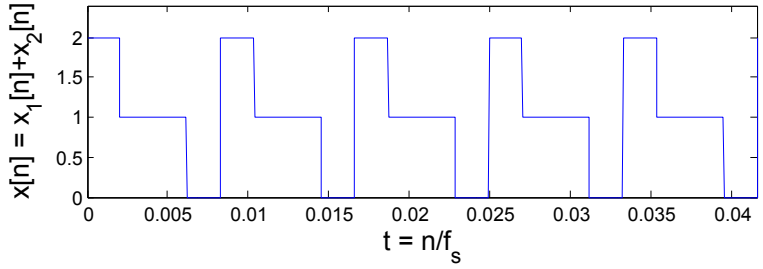

(c)

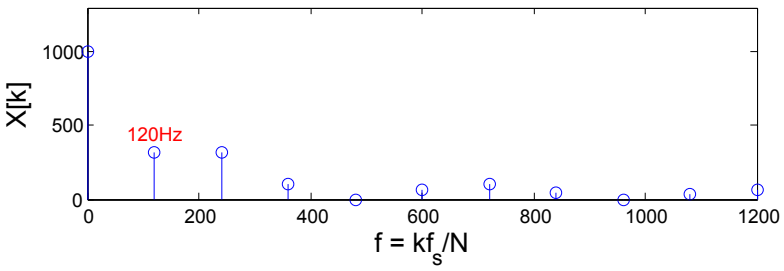

(d)

Figure 3: Here, we illustrate our concept for measuring the illuminance contribution of a single light source without causing any human-perceivable change in intensity. The first light source $x_1[n]$ (3a), is driven at 120 Hz with a 50% duty cycle. The second source $x_2[n]$ (3b) is driven at 240 Hz with a 50% duty cycle. An ideal receiver (no attentuation), measures the superposition of these two signals $x[n] = x_1[n] + x_2[n]$ (3c). Finally, an equivalent representation in the frequency domain is given (3d). The measurement $X[k]$ contains the information needed to characterize the attentuation of $x_1[n]$. Any effects of the rise and fall of the LED drivers and the LEDs themselves are ignored in this illustration.

of the sampled signal must be a multiple of one period; this means that an incomplete period of samples at the end of the signal must be removed before processing.

6. ESTIMATION OF MAXIMUM ILLUMINANCE

The previous section explained how to extract an approximate value of $|a_1|$ from the Fourier transform of the sampled signal $x[n]$. The next process is to calculate the PWM amplitude from the values of $|a_1|$ and the duty cycle. Assuming that the received PWM signals are perfect square waves, we can derive the precise analytical expression of the first Fourier series coefficient a_1 of the continuous-time signal $x(t)$. Suppose $x_1(t)$ is a PWM signal of amplitude E, duty cycle d, and period T.

$$x(t) = \begin{cases} E & nT \le t < (n+d)T \quad \text{for an integer } n \\ 0 & \text{otherwise} \end{cases} \tag{3}$$

Then, the first Fourier series coefficient can be calculated analytically as shown below.

$$\begin{aligned} a_1 &= \frac{1}{T}\int_0^T x(t)\ e^{-j\frac{2\pi t}{T}}\ dt \\ &= \frac{1}{2\pi}\int_{u_0}^{u_0+2\pi} x\left(\frac{Tu}{2\pi}\right)\ e^{-ju}\ du \quad \left(u = \frac{2\pi t}{T}\right) \\ &= \frac{1}{2\pi}\int_0^{2\pi d} Ee^{-ju}\ du \\ &= \frac{jE}{2\pi}\left(e^{-j2\pi d} - 1\right) \\ &= -\frac{jE}{\pi}\ e^{-j\pi d}\ \sin(\pi d) \\ \therefore \quad |a_1| &= \frac{E}{\pi}\ \sin(\pi d) \end{aligned} \tag{4}$$

Hence, we can plug the approximate value of $|a_1|$ into the relation $E = \pi|a_1|/\sin(\pi d)$ to estimate the PWM amplitude. Once the estimation process is repeated for all light fixtures, the linear program takes the result $E_1, E_2, \cdots$ as its coefficients to calculate the optimal PWM duty cycle values.

7. IMPLEMENTATION

In order to apply our new method to an actual lighting system, we wrote the mathematical procedures in MATLAB code. The code consists of three different functions: `find1stcoeff.m`, `findamplitude.m`, and `remcal.m`. The function `find1stcoeff.m` takes the sampled signal and its period and sampling frequency as its parameters and returns the approximate value of $|a_1|$. This function is recalled in `findamplitude.m`, where $|a_1|$ is used to determine the approximate value of the maximum illuminance E. Finally, `remcal.m` is a module which handles the calibration process, repeating the measurement for every light fixture. A diagram of a system using our new method is presented in Figure 4.

Our four-fixture system operates on an xPC Target procedure with the main controller in MATLAB connected via UDP. Since the new measurement method involves a signal at half the normal operation frequency, it required us to update the firmware which previously allowed us to run the light fixtures at a fixed frequency. A few technical difficulties with the firmware limited us to five different steps of duty cycle levels, but the test results were sufficient to show that our approach was valid.

In the process of choosing the values of the PWM signal frequency, we needed to ensure that the PWM frequency was fast enough so that the receiver buffer sampled at least one period of the whole signal. On the other hand, the frequency cannot be too high to maintain the resolution of the data, since the sampling frequency f_s of our detector (Fig. 1) was fixed at about 3.3 kHz. We picked the frequency to be 120 Hz under normal

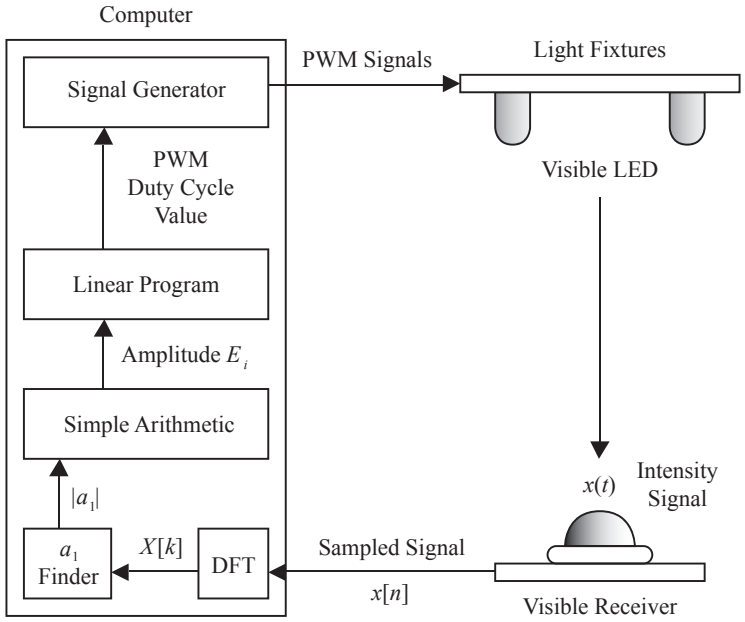

Figure 4: An updated data-flow diagram to include the calculation of the amplitude of the fundamental frequency $|a_1|$.

operation and 60 Hz during the calibration. This allowed us to have a little more than one full period in our 160-sample buffer and about 100 samples in one period.

One inevitable limitation of our method is that the system cannot perform the measurement with a binary signal. These constant signals do not include any harmonic component at nonzero frequency so the Fourier transform of these signals cannot give any information about the PWM amplitude. Therefore, the duty cycle values must have lower and upper limits in order to validate our method. Considering the accuracy and sampling rate of our receiver, the lower and upper limits of the PWM duty cycle must be greater than 5% from either the off set-point (binary 0) or the on set-point (binary 1). This factor, and the overall resolution of the pulse-width control for the light fixtures, limited us to only six possible brightness settings. Therefore, we tested using only six possible values: 0%, 20%, 40%, 60%, 80%, and 100%. Of those test points, only four possible values were used in testing after excluding 0% and 100%. However, we do not consider this problem as a critical limitation, as a custom designed LED driver and circuitry could provide finer PWM control indepedent of the fundamental frequency.

8. TESTING

To evaluate the system, we measure two unique illuminance profiles. The goal of the experiment is to study the effects of demodulating the light using our algorithm and contrast these results with the traditional method of turning on and off the light sources. This requires taking two measurements. The first measurement (Figure 5a), is the illuminance contributed by a single fixture at three different distances from the receiver using a 40% duty cycle. Here the units are arbitrary and given as counts from the analog to digital converter. In this case, we are interested in the difference between the minimum and maximum amplitudes measured by the receiver. These measurements represent the ideal illuminance E_t as measured by the receiver. Later, we will compare these results to those obtained by our technique.

In a perfect experiment, the measured difference between the maximum and minimum illuminance would be in exact agreement with the results of our algorithm. To determine if this is true, we test our algorithm by setting this same fixture to operate at 60 Hz and the rest of the light sources at 120 Hz. In this experiment we use the same 40% duty cycle as in the previous single-fixture test (Figure 5b). The 60 Hz signal operating at a 40% duty cycle is now embedded in the illuminance sample recorded by the receiver. We can demodulate

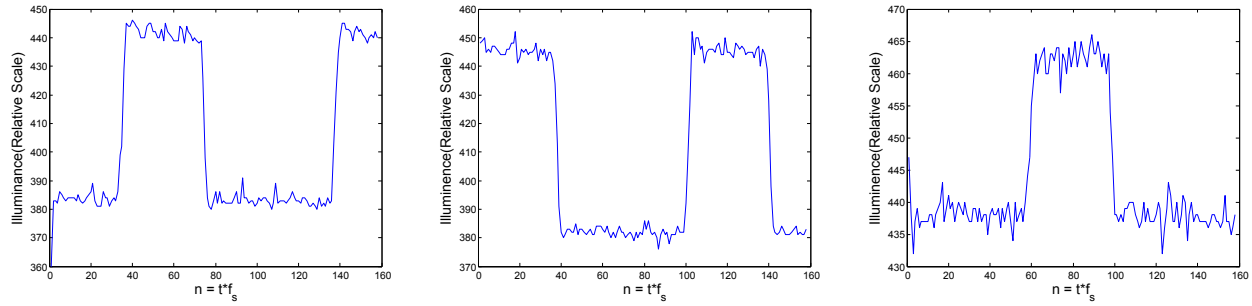

(a)

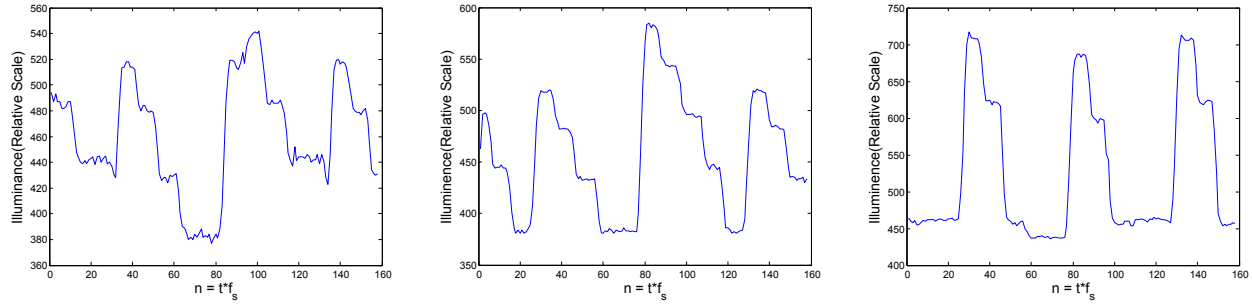

(b)

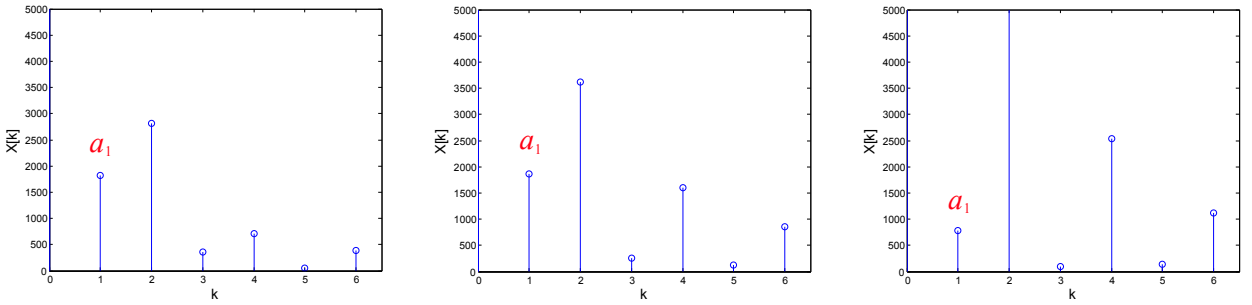

(c)

Figure 5: We present the results obtained from three experiments designed to measure the effectiveness of our new technique. We are interested in showing that the baseline measurement (E_t) and the results obtained from our algorithm ($\hat{E}_t$) are in agreement. First, we measure a 60 Hz signal driven at a 40% duty cycle at three different places under the testbed. This baseline illuminance E_t is measured with all controlled light sources set to off (5a). We repeat the experiment except that now, the three other light sources are driven at 120 Hz (5b). Finally, the coefficients $|a_1|$ are computed for the 60 Hz signal driven at 40% duty cycle (5c). The relationship of these coefficients to the estimated illuminance $\hat{E}_t$ are given in Eq. (4).

Table 1: The measured illuminance for a single luminaire (E_t) driven at 60 Hz and 40% duty cycle and the estimated illuminance ($\hat{E}_t$) using our demodulation techniques. The responses ΔE_t and $\Delta \hat{E}_t$ are obtained by calculating the difference between the minimum and maximum of the sample measured by the microcontroller. By calculating these parameters for all the light fixtures in the testbed, the relative contribution of each source at the target area is easily determined.

Measurement	Distance (cm)	ΔE_t (ADC Counts)	$\Delta \hat{E}_t$ (ADC Counts)
1	145	60	59
2	150	55	59
3	170	28	38

these data using Eq. (1) to obtain the magnitude of the first Fourier coefficient, $|a_1|$. This result is illustrated in Figure 5c. The remaining step requires using Eq. (4) to obtain $\hat{E}_t$, the estimated illuminance determined by our algorithm. As mentioned earlier, we are primarily interested in demonstrating that the difference between the maximum and minimum of the samples obtained in E_t and $\hat{E}_t$ are the same or very similar. Table 1 documents the results obtained in these two tests.

Overall, the technique performs as we expected, however angular sensitives of the receiver and the total resolution of the PWM control of the test fixtures contributed to the measurement error. In our third measurement (right, Fig. 5a) we see the error can be 25% for small amplitude signals (i.e., positioned far away from the detector, or a very low intensity). However, this accuracy issue does not invalidate our method, in that a light fixture with a smaller coefficient E_i has a smaller influence on the total illuminance at the receiver as well. We have also coded a sample controller using `remcal.m` in MATLAB and it behaved in the way we expected. The energy was optimized reasonably well and the coefficient estimates were consistent at a fixed location.

9. CONCLUSION

The new mathematical method featured in this paper provides us with a smooth update process of the user's location in a feedback controlled solid-state lighting system. Our new approach replaces the previous control system with the IR photoelectronic devices, minimizing the additional cost and the risk of side effect on the human eyes. The test results suggest that the accuracy of the measurement is actually better than in the IR system because visible light can afford much more illuminance without damaging the retina than infrared light can. We expect that this method can be applied to a more complicated lighting system involving multiple wavelengths, not just white LEDs. In this case, we have the possibility of monitoring the color temperature of an arbitrary luminaire without the need for sensing and measurement in the fixture itself.

ACKNOWLEDGMENTS

We wish to thank John Warwick and the team at Philips-Color Kinetics for the donation of the color-adjustable white fixtures for the control testbed. We also want to thank the Responsive Environments Group at the MIT Media Lab for their insight and help during testing. This research is directly funded by the MIT Media Lab.

REFERENCES

[1] Park, H., Burke, J., and Srivastava, M. B., "Design and implementation of a wireless sensor network for intelligent light control," in [*Proceedings of the 6th international conference on Information processing in sensor networks*], *IPSN'07*, 370–379, ACM (2007).

[2] Wen, Y. J., Granderson, J., and Agogino, A. M., "Towards embedded wireless-networked intelligent daylighting systems for commercial buildings," in [*Proceedings of the IEEE International Conference on Sensor Networks, Ubiquitous, and Trustworthy Computing*], *Proc. IEEE* **1**, 326–331, IEEE Computer Society (2006).

[3] Miki, M., Amamiya, A., and Hiroyasu, T., "Distributed optimal control of lighting based on stochastic hill climbing method with variable neighborhood," in [*Systems, Man and Cybernetics, 2007. ISIC. IEEE International Conference on*], 1676–1680, IEEE (2007).

[4] Pan, M.-S., Yeh, L.-W., Chen, Y.-A., Lin, Y.-H., and Tseng, Y.-C., "Design and implementation of a wsn-based intelligent light control system," *Distributed Computing Systems Workshops, International Conference on* **0**, 321–326 (2008).

[5] Schubert, E. F. and Kim, J. K., "Solid-state light sources getting smart," *Science* **308**(5726), 1274–1278 (2005).

[6] Caicedo, D., Pandharipande, A., and Leus, G., "Occupancy-based illumination control of LED lighting systems," *Lighting Research and Technology* (2010).

[7] Aldrich, M., Zhao, N., and Paradiso, J., "Energy efficient control of polychromatic solid state lighting using a sensor network," in [*Proceedings of SPIE*], **7784**, 778408 (2010).

[8] Wen, Y. and Agogino, A., "Control of wireless-networked lighting in open-plan offices," *Lighting Research and Technology* (2010).

[9] Bhardwaj, S., Ozcelebi, T., and Lukkien, J., "Smart lighting using LED luminaries," in [*Pervasive Computing and Communications Workshops (PERCOM Workshops), 2010 8th IEEE International Conference on*], 654–659, IEEE (2010).